Journal of Geophysical Research: Space Physics

Supporting Information for

Characterizing Precipitation Behaviors of H^- in the Martian Atmosphere

Sarah Henderson[1,2], Jasper Halekas[1], Rebecca Jolitz[3], David Mitchell[3], Christian Mazelle[4], Frank Eparvier[5], Meredith Elrod[6]

[1] The University of Iowa, Iowa City, IA, USA
[2] Montana State University, Bozeman, MT, USA
[3] Space Sciences Laboratory, University of California Berkeley, Berkeley, CA, USA
[4] IRAP, Université de Toulouse, CNRS, UPS, CNES, Toulouse, France
[5] Laboratory for Atmospheric and Space Physics, University of Colorado, Boulder, CO, USA
[6] Planetary Environments Lab, Goddard Space Flight Center, NASA, Greenbelt, MD, USA
[7] CRESST II, University of Maryland, College Park, College Park, MD, USA

Contents of this file

Figures S1, S2, and S3.

Introduction

This supporting document includes figures outlining parameters implemented in various calculations throughout our manuscript. Here, we include a plot summarizing photodetachment and photoabsorption cross section curves as a function of energy. These values were utilized in our calculations in Section 3.1. We also include an average CO_2 profile derived from dayside, inbound verified NGIMS data. We fit an exponentially decaying function to these average data and note the fitting parameters (N_0 and m) in our plot. These fit parameters were implemented in calculations in Sections 3.2, 3.2.1, and 3.2.2. We also include a summary of the differences between the numerical modeling results discussed in Section 3.2 at different Mars-Sun distances.

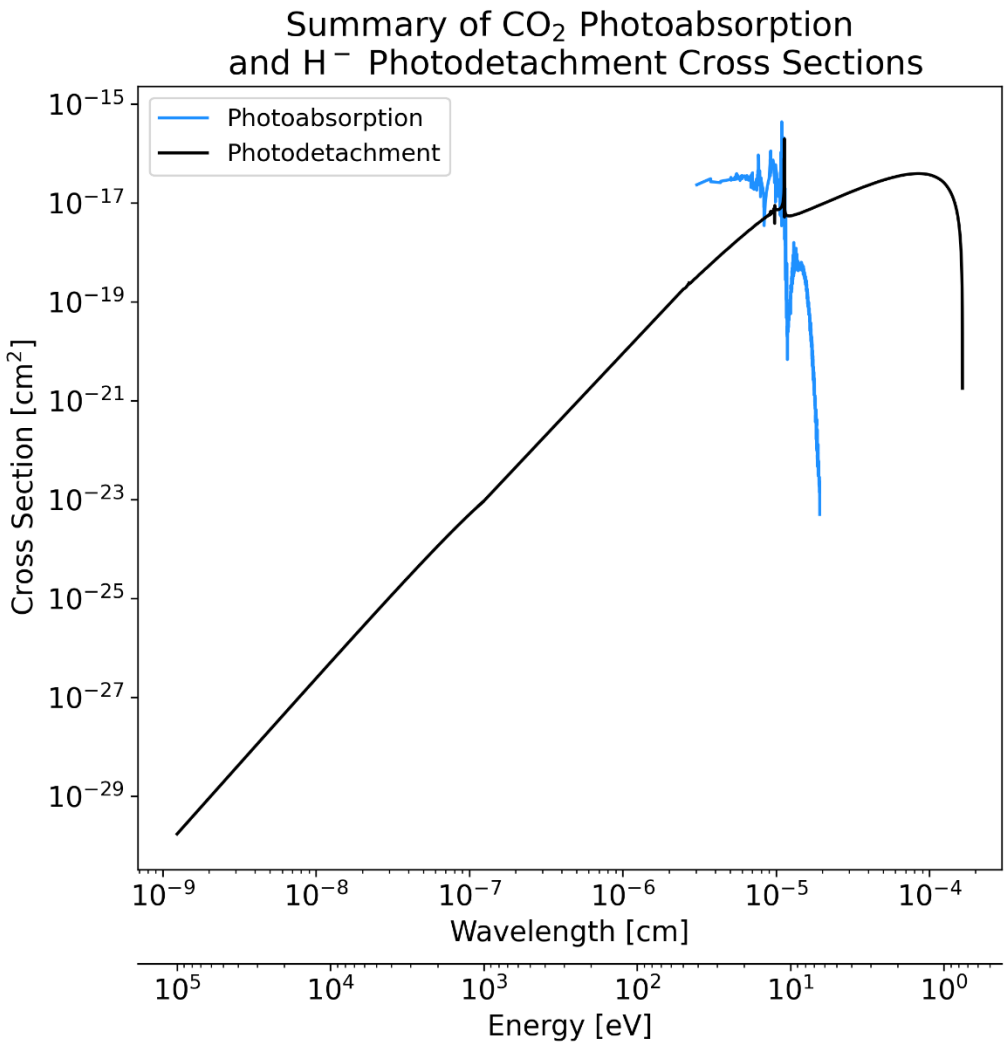

Figure S1. Summary of CO_2 photoabsorption and H^- photodetachment cross sections. EUV photoabsorption cross sections compiled from numerous sources (Sun & Weissler, 1955; Cairns & Samson, 1965; Lewis & Carver, 1983; Yoshino et al., 1996; Parkinson et al., 2003; Stark et al., 2007). Photodetachment cross sections from McLaughlin et al. (2017) and sources therein.

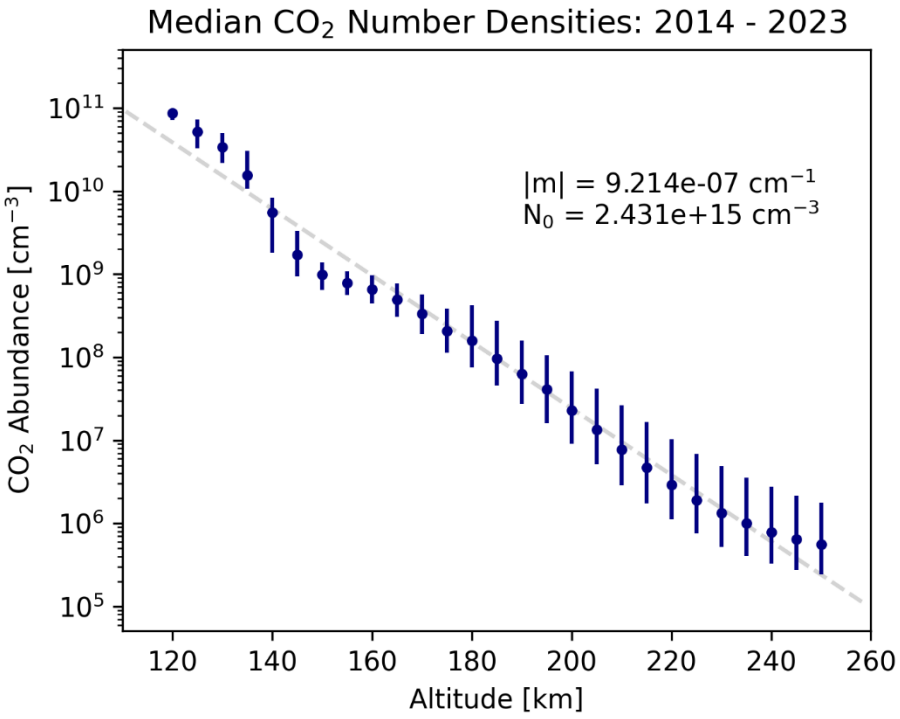

Figure S2. Median CO_2 density profile from inbound verified dayside NGIMS data collected between 2014 and 2023 with interquartile ranges Q1 and Q3 as lower and upper error bars, respectively. Fit parameters, N_0 and m, are in the upper right corner. Resulting fit overplotted in gray, dashed line.

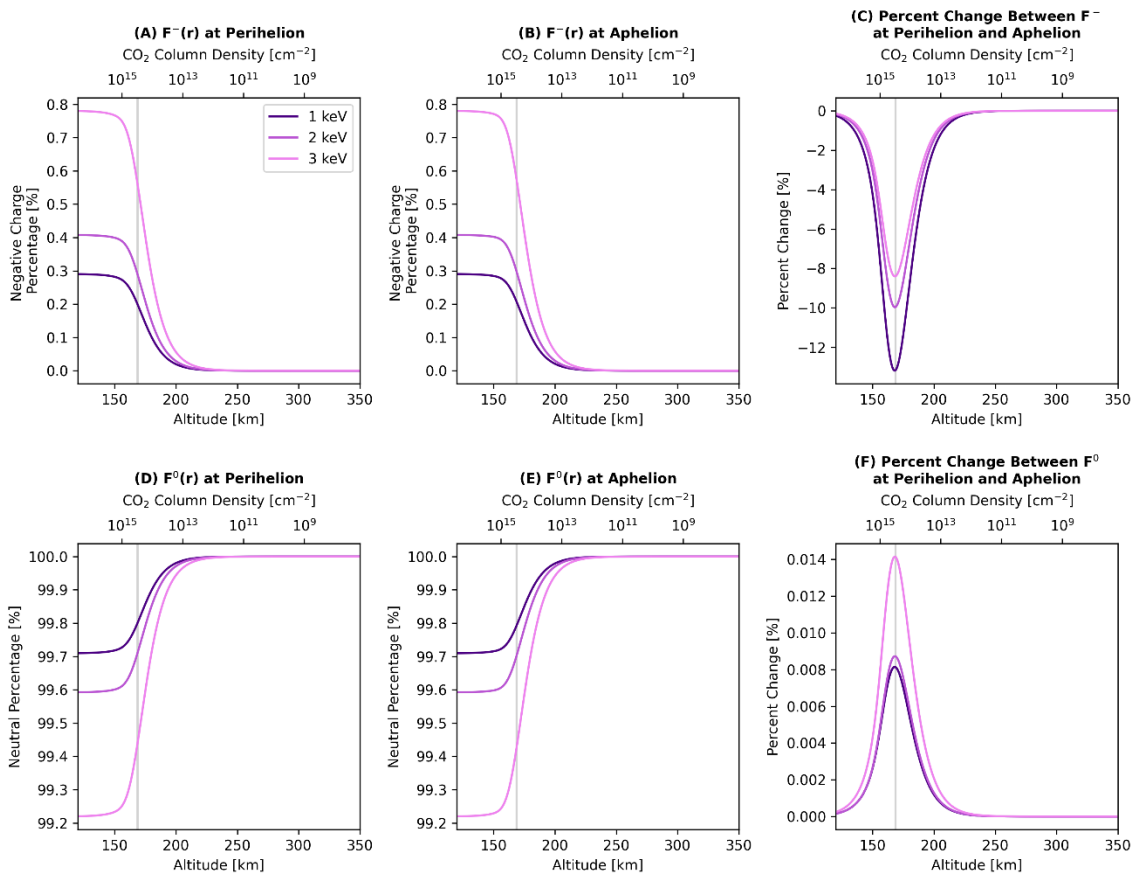

Figure S3. Summary of numerical solutions to Equations 19 and 20 at different Mars-Sun distances. (A) Negative charge fraction (F^-) versus altitude and column density for upstream solar wind energies of 1, 2, and 3 keV at perihelion. (B) Same as Panel A but at aphelion. (C) Percent change ($c = 100\ [F^-_{PER} - F^-_{AP}]/\ F^-_{AP}$) between F^- at perihelion and aphelion for each solar wind energy. Panels D - F follow this format but display the neutral fraction (F^0) solutions. Gray vertical region in each subpanel highlights the equilibrium column density range (i.e., where one e-folding occurs in Equations 27 and 28). It should be noted that no atmospheric changes between aphelion and perihelion were incorporated in these results; only the changes induced by the Mars-Sun distance dependence in Equations 19 and 20 are displayed here.